Molecular order and dynamics in planar lipid bilayers: Effects of unsaturation and sterols

ARTICLE *in* BIOCHEMISTRY · MARCH 1988

Impact Factor: 3.02 · DOI: 10.1021/bi00403a003 · Source: PubMed

4 AUTHORS, INCLUDING:

Herman van Langen
VieCuri Medical Center Noord-Limburg
67 PUBLICATIONS **1,179** CITATIONS
SEE PROFILE

Gijs Van Ginkel
Utrecht University
70 PUBLICATIONS **1,811** CITATIONS
SEE PROFILE

Articles

Molecular Order and Dynamics in Planar Lipid Bilayers: Effects of Unsaturation and Sterols

Geurt Deinum, Herman van Langen, Gijs van Ginkel,* and Yehudi K. Levine
Department of Molecular Biophysics, Laboratory of Experimental Physics, Rijksuniversiteit Utrecht, Princetonplein 5, 3584 CC Utrecht, The Netherlands

Received June 12, 1987; Revised Manuscript Received September 29, 1987

ABSTRACT: Angle-resolved fluorescence depolarization experiments were carried out on 1,6-diphenyl-1,3,5-hexatriene (DPH) and 1-[4-(trimethylammonio)phenyl]-6-phenyl-1,3,5-hexatriene (TMA-DPH) molecules embedded in macroscopically oriented multilayers of saturated [dimyristoylphosphatidylcholine (DMPC)] and unsaturated [palmitoyloleoylphosphatidylcholine (POPC), dioleoylphosphatidylcholine (DOPC), dilineoylphosphatidylcholine (DLPC), plant digalactosyldiglyceride (DGDG)] lipids with and without cholesterol. In all the lipid systems studied the order parameter $\langle P_2 \rangle$ of TMA-DPH molecules was found to be higher than that for DPH. Considerations of the order parameter $\langle P_4 \rangle$, however, indicate that DPH molecules have a heterogeneous distribution in bilayers of unsaturated lipids, with a significant fraction of the molecules lying with their long axes parallel to the bilayer planes. Both the DPH and TMA-DPH molecules exhibit a decrease in the molecular order as well as a decrease in their rates of motion on increasing the unsaturation of the hydrocarbon chains. The addition of cholesterol tends to reverse this effect, with an increase in both the order and dynamics. Bilayers of DOPC, however, exhibit a somewhat different result. It is suggested that the discrepancies between these observations and findings with lipid vesicle systems simply reflect the effects of curvature on the behavior of the probe molecules. The results indicate that the concept of membrane fluidity must be used with great caution.

Physical techniques are widely used in quantitative studies of the nature of the interactions between and the structural roles of phospholipids, cholesterol, and proteins in membrane systems (Quinn & Chapman, 1980; Seelig & Seelig, 1980; Huang, 1977; Yeagle, 1985; Stubbs, 1983). The experimental results are often interpreted in terms of "membrane fluidity", which is now taken to be a general concept describing the overall physical state of the membrane system and in particular the lipid bilayer. Seelig and Seelig (1980) have pointed out that in order to define the physical state of the membrane lipids on a molecular level one has to distinguish clearly between the time-averaged structural parameters, such as order parameters, and the relaxation times or correlation times, which characterize the dynamics and fluctuations in the structure. The correlation between the molecular order and the dynamics of the lipid fatty acid chains is, however, as yet not well understood.

Studies of model membrane systems have shown that the molecular order and dynamics of the lipid chains are drastically affected by the introduction of cis double bonds into the fatty acid chains of the lipid molecules. It is now commonly accepted that the introduction of unsaturation results in a marked decrease of the molecular order in the liquid-crystalline phases of the lipids (Seelig & Seelig, 1977; Stubbs et al., 1981; van de Ven & Levine, 1984; Mulders et al., 1986). However, deuterium NMR[1] investigations of Seelig and co-workers (Seelig & Seelig, 1975; Seelig & Waespe-Šarčevic, 1978) have shown that the effects of geometric factors have to be considered in the interpretation of NMR data. If this was done, they found no reduction in membrane order with the introduction of a double bond in the membrane.

ESR[1] experiments (Seelig & Seelig, 1977) and time-resolved fluorescence anisotropy studies (Stubbs et al., 1981) of probes embedded in vesicle systems have shown that the introduction of cis double bonds into the lipid chains causes an increase in the dynamics of the probes. In marked contrast, ESR experiments (Koole et al., 1984; Van Ginkel et al., 1986) and fluorescence depolarization experiments (Van de Ven & Levine, 1984; Mulders et al., 1986) report slower orientational motions of the probe molecules in multibilayer systems of unsaturated lipids than in multibilayers of DMPC above their phase transition.

The effects of cholesterol on the properties of model membranes have also been the subject of much research effort [for a review, see Yeagle (1985)]. It has been shown, by a variety of techniques, that the addition of cholesterol into phospholipid bilayers enhances the orientational order of the hydrocarbon chains in the fluid-crystalline phase but disrupts it in the gel phase (Dufourc & Smith, 1986; Dufourc et al., 1984; Kusumi et al., 1986; Guyer & Bloch, 1983; Wolber & Hudson, 1981; Yeagle, 1981; Johansson & Lindblom, 1980; Kawato et al., 1978; Huang, 1977; Demel & De Kruijff, 1976). It is currently accepted that in the presence of cholesterol the acyl chain region of the lipid bilayer is in a state intermediate between the gel and liquid-crystalline phases (Yeagle, 1985). The steroid nucleus of the cholesterol molecule is rigid and bulky, and there are strong experimental indications that it overlaps the first 9-12 carbons of the lipid chains, thus restricting their motion; the terminal sections of the chains are

[1] Abbreviations: PC, phosphatidylcholine; DMPC, 1,2-dimyristoyl-*sn*-glycero-3-phosphocholine; POPC, 1-palmitoyl-2-oleoyl-*sn*-glycero-3-phosphocholine; DOPC, 1,2-dioleoyl-*sn*-glycero-3-phosphocholine; DLPC, 1,2-dilineoyl-*sn*-glycero-3-phosphocholine; DGDG, digalactosyldiacylglycerol; DPH, 1,6-diphenyl-1,3,5-hexatriene; TMA-DPH, 1-[4-(trimethylammonio)phenyl]-6-phenyl-1,3,5-hexatriene; NMR, nuclear magnetic resonance; ESR, electron spin resonance.

0006-2960/88/0427-0852$01.50/0

then less affected (Oldfield et al., 1978; Dufourc et al., 1984; Stockton & Smith, 1976; Kutchai et al., 1983). Unsaturated acyl chains, however, appear to have a different interaction with cholesterol than saturated ones (Kusumi et al., 1986; Demel et al., 1972). The ordering influence of cholesterol in bilayers of unsaturated lipids was found to be greatly reduced compared to bilayers of saturated lipids. Monolayer studies (Demel et al., 1972) showed that the addition of cholesterol to monolayers of disaturated or di-unsaturated acyl chains had no condensation effects. Monolayers of mixed-chain phosphatidylcholines did, however, exhibit condensation whereby the mean area per molecule decreased significantly. Huang (1977) explained these observations by assuming that the β surface of the sterol nucleus interacts preferentially with the "pocket" above the $\Delta_{9,10}$-cis double bond of the acyl chain, while the α face interacts preferentially with the fully saturated chains.

Although the influence of cholesterol on the molecular order in bilayer systems is clear-cut, the consequences for the molecular dynamics as monitored by fluorescence depolarization experiments appear to be confused (Kawato et al., 1977; Veatch & Stryer, 1977; Hildenbrand & Nicolau, 1979; Wolber & Hudson, 1981; Kutchai et al., 1983). Interestingly, Ghosh and Seelig (1982) have shown using ^{2}H NMR experiments that the addition of cholesterol to bilayers of different phosphatidylethanolamines induces a dramatic increase in the T_1 values, which correspond to increases in the rates of motion of the trans double bonds of the acyl chains.

Here we report a study of the molecular order and dynamics of the fluorescent probe molecules DPH and TMA-DPH embedded in bilayers of unsaturated lipids with or without cholesterol. The aim of the study is to clarify the correlations between the orientational order and reorientational dynamics in multibilayer systems induced both by an increase of the unsaturation of the hydrocarbon chains and by the addition of cholesterol. The technique of steady-state angle-resolved fluorescence depolarization (AFD) was used in the experiments (Van der Meer et al., 1982; Kooyman et al., 1983; Van de Ven & Levine, 1984; Mulders et al., 1986; Van Ginkel et al., 1986). We have shown previously that measurements of the angle-resolved fluorescence depolarization combined with knowledge of the fluorescence decay functions afford the determination of the order and dynamics of the probe molecules in lipid bilayer systems (Mulders et al., 1986; Van Ginkel et al., 1986). Furthermore, the order parameters of the absorption and emission transition moments of the probes are also easily determined. The value of the technique in studies of lipid bilayer systems has been amply demonstrated.

The results show that DPH molecules possess a heterogeneous orientational distribution in bilayers of unsaturated lipids, with a significant fraction of the molecules lying with their long axes parallel to the bilayer planes. This is in marked contrast to TMA-DPH molecules, which in any case are expected to be anchored at the head group region of the bilayer. Both the DPH and TMA-DPH molecules exhibit a decrease in the molecular order as well as a decrease in their rates of motion on increasing the unsaturation of the hydrocarbon chains. The addition of cholesterol merely reverses this trend and causes an increase in both the order and dynamics. Bilayers of DOPC, however, exhibit a somewhat different behavior.

It is concluded that the discrepancies between these findings and the results from small unilamellar lipid vesicles simply reflect the effects of curvature on the behavior of the probe molecules. The results thus indicate that the concept of membrane fluidity must be used with great caution.

Theory

Angle-Resolved Fluorescence Depolarization (AFD) Experiments. The theory of the experiment has been discussed in detail previously (Van der Meer et al., 1982; Kooyman et al., 1983; Van de Ven & Levine, 1984) and will only be summarized here. The experimental geometry described by Van de Ven and Levine (1984) and Mulders et al. (1986) was employed. The angle-resolved fluorescence depolarization ratios are given by

$$R_e = I_\perp/I_\parallel = [1 - R_1 + (R_3 + R_1)\sin^2\theta]/ [1 + R_1 + (R_2 - R_1)\sin^2\phi + (R_3 - R_1)\sin^2\phi + R_4 \sin 2\theta \sin 2\phi + R_5 \sin^2\phi \sin^2\theta] \quad (1)$$

where $I_\perp$ and $I_\parallel$ are the intensities of the fluorescence emission polarized respectively perpendicular to and parallel to the plane of incidence. Here θ denotes the angle of incidence of the excitation beam relative to the normal (director) to the multibilayer plane, and ϕ is the angle under which the light emission is observed. The only assumption underlying the derivation of eq 1 is that the probe molecules have a macroscopically uniaxial distribution about the normal to the surface of the sample.

The angles in the sample and the laboratory can be related simply if the refractive index of the same is known. However, the effects of the sample/air interface on the transmission of light intensity are more complex and depend furthermore on the direction of polarization. The various artifacts have been discussed in detail by Lax and Nelson (1973). It can be easily shown that the effects of multiple reflections of the exciting and emitted light within the sample compensate the transmission losses of the fluorescent light at the interface. Furthermore, consideration of the ϕ dependence of the intensities $I_\perp$ and $I_\parallel$ obtained with a normal incidence of the exciting light ($\theta = 0°$) indicates that only solid-angle expansion [see Lax and Nelson (1973)] distorts the experimental results. This effect cancels out on calculating the polarization ratio. Consequently, no correction need be applied to the values of R_e determined experimentally. We note here that Van de Ven and Levine (1984) ignored the effects of multiple reflections in the analysis of their results.

The polarization ratio R_e is measured for various combinations of θ and ϕ and affords the determination of five independent quantities, S_μ, S_ν, g_0, g_1, and g_2, from steady-state experiments. Here S_μ and S_ν are respectively the second rank order parameter ($\equiv\langle P_2\rangle$) for the absorption and emission transition moments. For DPH and TMA-DPH molecules the quantities g_k, $k = 0$, 1, and 2, are defined by

$$g_k = 2.5 r_0 \int_0^\infty G_k(t)\, dt$$

$$G_k(t) = \langle D^2_{k0}(\Omega_\mu) D^{2*}_{k0}(\Omega_\nu)\rangle$$

$$\int_0^\infty F(t)\, dt = \int_0^\infty \{(\alpha_1/\tau_1)\exp(-t/\tau_1) + (\alpha_2/\tau_2)\exp(-t/\tau_2)\}\, dt = 1 \quad (2)$$

where D^2_{k1} are Wigner rotation matrix elements (Rose, 1957) and Ω_μ and Ω_ν denote respectively the orientation of the absorption moment at time $t = 0$ and that of the emission moment at time t, relative to the director frame. $F(t)$ denotes the normalized intrinsic fluorescence decay function, and r_0 is the fundamental anisotropy of the molecules.

The time behavior of the correlation functions $G_k(t)$ is obtained from models for the reorientational motion of the

molecules. It is important to realize that the values of $G_k(t)$ for $t = 0$ and $t \rightarrow \infty$ are model independent as a consequence of the assumption that the motion can be described as a stochastic process. These limits can be expressed solely in terms of the order parameters $\langle P_2 \rangle$ and $\langle P_4 \rangle$ (Zannoni et al., 1983; Zannoni, 1979). The correlation functions $G_1(t)$ and $G_2(t)$ decay to zero at long time, whereas the function $G_0(t)$ decays to a constant value given by $\langle P_2 \rangle^2$.

$F(t)$ can be determined experimentally on observing the fluorescence emission in a direction normal to the sample surface ($\phi = 0°$) and under an angle of incidence in the sample of $\theta = \sin^{-1}(1/\sqrt{3})$. If the polarizer on the emission side is set with its optical axis at 45° to the vertical, then the combined signal $I_\perp + I_\parallel$ is proportional to $F(t)$ (Van der Meer et al., 1982).

Orientation of Molecules in Membrane Systems. We shall here consider the case of a uniaxial bilayer system containing cylindrically symmetric probe molecules. The orientation of the molecules in the system is specified by the angle β between the molecular symmetry axes and the bilayer normal (Zannoni, 1981).

The orientational distribution of an average molecule in the system is then characterized by a probability distribution $f(\beta)$. This distribution can be expressed as a series expansion of Legendre polynomials, $P_L(\cos \beta)$, each of which is weighted by an order parameter $\langle P_L \rangle$ which is the ensemble average of the corresponding term:

$$f(\beta) = (1/2) \sum_{L=0}^{\infty} (2L + 1) \langle P_L \rangle P_L(\cos \beta) \qquad L \text{ even} \quad (3)$$

$$f(\beta) \geq 0; \int_0^\pi f(\beta) \sin \beta \, d\beta = 1$$

$$\langle P_L \rangle = \int_0^\pi f(\beta) P_L(\cos \beta) \sin \beta \, d\beta$$

The orientational distribution function $f(\beta)$ is fully characterized if all the order parameters $\langle P_L \rangle$ are known. In practice, however, only $\langle P_2 \rangle$ and $\langle P_4 \rangle$ are accessible experimentally. Mathematically, $\langle P_2 \rangle$ and $\langle P_4 \rangle$ are defined as

$$\langle P_2 \rangle = (1/2) \langle 3 \cos^2 \beta - 1 \rangle$$

$$\langle P_4 \rangle = (1/8) \langle 35 \cos^4 \beta - 30 \cos^2 \beta + 3 \rangle$$

The main difficulty now is obtaining an objective and realistic estimate of the form of $f(\beta)$ from limited knowledge of its moments. This may be accomplished by an information-theoretic approach (Van der Meer et al., 1982). The essential point is that, given the order parameters $\langle P_2 \rangle$ and $\langle P_4 \rangle$, the most probable values of $\langle P_L \rangle$, $L \geq 6$, are calculated under the assumption that the informational entropy of $f(\beta)$ is a maximum. This corresponds to the construction of the broadest possible distribution function consistent with the known values of $\langle P_2 \rangle$ and $\langle P_4 \rangle$. It can then be shown that the resulting distribution function has the form

$$f(\beta) = A \exp[\lambda_2 P_2(\cos \beta) + \lambda_4 P_4(\cos \beta)] \quad (4)$$

where A is a normalization constant and λ_2 and λ_4 are determined from the known values of $\langle P_2 \rangle$ and $\langle P_4 \rangle$. If only the order parameter $\langle P_2 \rangle$ is known, the distribution function takes the form of eq 4 but with $\lambda_4 = 0$. We note here that eq 4 has the form of a Boltzmann distribution with an angle-dependent orienting potential.

It can be seen from eq 4 that if only $\langle P_2 \rangle$ is known, the reconstructed distribution function has either a maximum at $\beta = 0$ and decreases monotonically to a minimum at $\beta = \pi/2$ or vice versa. Knowledge of $\langle P_4 \rangle$ is required for establishing the existence of a collective molecular tilt which is manifested by a maximum of the distribution function at an angle intermediate between 0 and $\pi/2$. On the other hand the observation of a minimum at such an angle may be taken as an indication for a superposition of two or more independent populations of molecules. The available information, however, is too limited to allow their resolution.

Model for Reorientational Motion: The Rotational Diffusion Model. The probe molecules in this model are assumed to undergo small-step rotational diffusion subject to an anisotropic orienting potential $U(\beta)$. In view of the discussion above on the reconstruction of the equilibrium orientation distribution function, we shall choose $U(\beta)$ to take the form

$$U(\beta) = -kT\{\lambda_2 P_2(\cos \beta) + \lambda_4 P_4(\cos \beta)\} \quad (5)$$

We note that our choice of the orienting potential spans all the physically permissible pairs of ($\langle P_2 \rangle$, $\langle P_4 \rangle$) values. It is important to realize that this model does not presuppose sticky boundary conditions for which an interpretation in terms of viscosity is valid.

The correlation functions are now given as a sum of exponential decays:

$$G_k(t) = \sum_M b_M^k \exp(-D_\perp \alpha_M^k t) \quad (6)$$

where the amplitudes b_M^k and the exponential factors α_M^k are determined by λ_2 and λ_4. $D_\perp$ is the diffusion coefficient of the symmetry axis of the molecule.

In many practical situations, the correlation functions $G_k(t)$ are found to have a monoexponential decay of the form of eq 5 but with a separate correlation time for each k (Zannoni et al., 1983; Szabo, 1984).

Materials and Methods

Cholesterol, dimyristoylphosphatidylcholine (DMPC), palmitoyloleoylphosphatidylcholine (POPC), dioleoylphosphatidylcholine (DOPC), and dilineoylphosphatidylcholine (DLPC) were purchased from Sigma Chemical Co. (St. Louis, MO) and used without further purification. Plant digalactosyldiacylglycerol (DGDG) was bought from Lipid Products (England). Stigmasterol and 1,6-diphenyl-1,3,5-hexatriene (DPH) were obtained from Fluka (Switzerland). TMA-DPH was purchased from Molecular Probes Inc. (Plano, TX). The fluorescent probes were dissolved in absolute ethanol and stored under nitrogen in the dark at 4 °C. When necessary, the purity of the lipids and the fluorescence probes were controlled by HPTLC.

Sample Preparation. Lipid bilayers macroscopically oriented between microscope coverglasses were prepared as described by Kooyman et al. (1983), Van de Ven and Levine (1984), and Mulders et al. (1986). Perfectly aligned samples were selected by means of a polarization microscope equipped with a first-order red plate, and it was checked that the same values of the polarization ratio R_e, within the experimental error of 2%, were obtained on rotating the samples by an arbitrary angle about the normal to their surfaces.

DPH and TMA-DPH were used as fluorescent probes; the probe to lipid ratio was 1:250 on a molecular basis. The membrane systems were kept in the dark as much as possible and were only exposed to daylight during the alignment procedure and on being mounted in the sample holder. Since the lipids used in these investigations are highly susceptible to oxidation, all manipulations were performed as much as possible in a nitrogen atmosphere. The sample contained ca. 25% water unless otherwise stated.

Table I: Typical Examples of Deconvolution of the Fluorescence Decay of DPH and TMA-DPH in Different Lipid Bilayers

lipid + probe	χ^2_r	α_1	τ_1 (ns)	α_2	τ_2 (ns)	$\langle\tau_F\rangle$	T (°C)
DMPC + DPH						8.21[b]	35
POPC + DPH	1.17	0.059	2.99	0.941	7.87	7.58	21
DOPC + DPH	1.74	0.100	0.72	0.900	7.34	6.68	21
DLPC + DPH	1.37	0.095	2.64	0.905	7.34	6.90	21
DGDG + DPH							21
DMPC + chol + DPH							35
POPC + chol + DPH	1.16	0.080	1.19	0.920	7.48	6.97	21
DOPC + chol + DPH	1.28	0.064	1.75	0.936	7.48	7.11	21
DLPC + chol + DPH	1.16	0.085	2.29	0.915	7.29	6.86	21
DGDG + chol + DPH							21
DMPC + TMA						5.8[b]	35
POPC + TMA	1.71	0.158	1.66	0.842	5.14	4.59	21
DOPC + TMA	1.28	0.313	1.06	0.687	3.95	3.04	21
DLPC + TMA	1.39	0.297	1.51	0.703	4.55	3.65	21
DGDG + TMA	2.73	0.218	0.94	0.782	3.07	2.60	21
DMPC + chol + TMA	1.03	0.054	0.87	0.946	6.08	5.80	35
POPC + chol + TMA	1.03	0.072	1.65	0.928	5.76	5.47	21
DOPC + chol + TMA	1.26	0.230	1.51	0.770	4.94	4.15	21
DLPO + chol + TMA	1.41	0.368	1.46	0.632	4.52	3.40	21
DGDG + chol + TMA	1.29	0.597	1.32	0.403	5.16	2.87	21

[a] The analysis is presented in terms of the following parameters: τ_1, fluorescence lifetime of component 1; τ_2, fluorescence lifetime of component 2; $\langle\tau_F\rangle$, average fluorescence lifetime, which is defined as $\alpha_1\tau_1 + \alpha_2\tau_2$, where $\alpha_1 + \alpha_2 = 1$; χ^2_r, reduced χ^2, a measure for the goodness of fit between the observed data points and the calculated ones. If χ^2_r is less than or close to unity, the fitting function can be considered appropriate; see Dale et al. (1977) and Dale (1980). [b] Data taken from Mulders et al. (1986).

As the unsaturation in the fatty acyl chains increased, it became more difficult to obtain well-aligned samples in the presence of cholesterol. Crystal-like structures were observed at times, and such preparations were discarded. Similar crystallization effects were observed with stigmasterol and β-sitosterol.

AFD Measurements. Angle-resolved fluorescence depolarization experiments were carried out with the home-built fluorometer described by Mulders et al. (1986). Fluorescence decay measurements were carried out with a similar experimental setup as used for the steady-state AFD experiments using the synchrotron in Daresbury (England) as a pulsed light source. Time-resolved fluorescence emission was measured by a single photon counting detection system (Ortec) equipped with a Philips XP2020Q photomultiplier tube (Mullard House, London, England). DPH and TMA-DPH were excited at 363 nm, and their fluorescence emission was measured at 435 nm with the optical equipment described by Mulders et al. (1986).

The fluorescence decay function was extracted from the measurements using reiterative nonlinear least-squares deconvolution methods following Dale et al. (1977). The best fit was judged by the χ^2 test, distribution of residuals, and their correlation function was mostly obtained for a biexponential decay.

The intensity of the exciting light was kept as low as possible to avoid bleaching of the probe molecules, and the intensity of fluorescence, measured at the same scattering geometry, remained constant during the experiments. Control experiments showed that the intrinsic fluorescence signals from the lipids and the coverslips amounted to <1% of the probe fluorescence intensity.

Results

AFD experiments were carried out on DPH and TMA-DPH molecules embedded in multibilayers of DMPC, POPC, DOPC, DLPC, and DGDG with and without cholesterol. In addition, multibilayers of POPC and DGDG containing stigmasterol and DPH were also studied. The same values of the polarization ratios R_e, within the experimental error of 2%, were obtained on rotating the samples by an arbitrary angle about the normal to their planes. This indicates that the probe molecules possessed a uniaxial distribution in the samples. The results shown represent an average of at least five different samples of each system. The fluorescence depolarization ratios were measured for 56 different combinations of the angles θ and ϕ. The fluorescence decay functions obtained from the deconvolution procedures with biexponential decays are shown in Table I.

Data Analysis. The experimentally observed depolarization ratios were fitted directly in terms of the rotational diffusion model following the procedure described by us previously (Van Ginkel et al., 1986; Mulders et al., 1986) and with the normalized fluorescence decay functions $F(t)$ shown in Table I.

The analysis makes use of two of our previous findings (Van Ginkel et al., 1986; Mulders et al., 1986; Van de Ven & Levine, 1984; Kooyman et al., 1983). Experiments on macroscopically ordered multibilayer systems indicate consistently that the order parameter S_μ of the absorption transition moment is significantly higher than S_ν, the order parameter of the emission transition moment of DPH and TMA-DPH. This observation on DPH was corrobarated by Johansson (1985) in other oriented lipid systems. We have shown that this can be explained simply on taking the absorption moment to lie parallel to the long molecular axis of the molecule, but with the emission moment making an angle β_ν relative to that axis. Second, we have shown (Van Ginkel et al., 1986; Mulders et al., 1986) that the AFD experiment is only sensitive to the long life time component of the fluorescence decay. Consequently, the experimental results can be interpreted, with negligible error, on taking the fluorescence decay to be monoexponential with an effective life-time equal to $\langle\tau\rangle$, where

$$\langle\tau_f\rangle = \int_0^\infty tF(t)\,dt \qquad (7)$$

These same considerations are valid for the systems reported here.

The experimental data were analyzed with $D_\perp\langle\tau_F\rangle$, λ_2, λ_4, and $P_2(\cos\beta_\nu)$ as free model parameters. Analyses of the results with $\lambda_4 = 0$ were also attempted but yielded unsatisfactory fits with systematic deviations for systems containing DPH molecules. Reasonable fits were obtained for the TMA-DPH results, though these still exhibited some systematic discrepancies. This is in accord with previous results on other lipid systems (Van Ginkel et al., 1986; Mulders et al.,

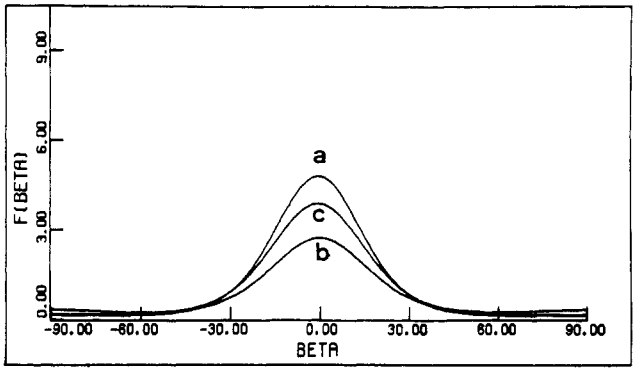

FIGURE 1: Orientational distribution functions of DPH molecules in multibilayers of POPC (a), DOPC (b), and DLPC (c).

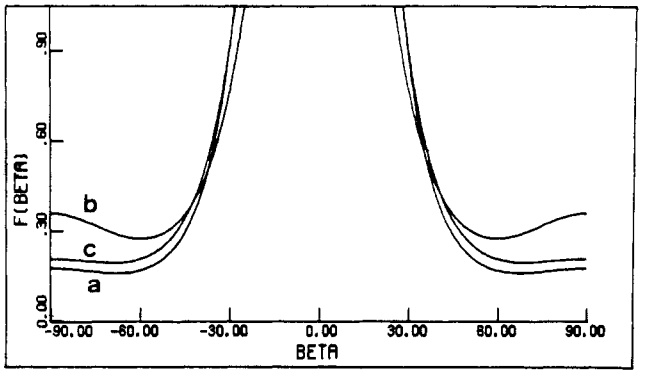

FIGURE 2: Orientational distribution functions of Figure 1 enlarged 10 times to show the population of DPH molecules in multibilayers of POPC (a), DOPC (b), and DLPC (c) at 90 °C.

1986). The best fit parameters are shown in Table II, together with the derived order parameters $\langle P_2 \rangle$ and $\langle P_4 \rangle$. We have, unfortunately, been unable to analyze the results of the DMPC + cholesterol systems, which yielded high depolarization ratios as a consequence of the near perfect orientational order of the probe molecules.

The analysis shows that the angle β_v between the absorption and emission moments of DPH is large (≈30°) and varies with the chemical composition of the system. In marked contrast, much smaller angles were obtained for TMA-DPH (≈16°). Furthermore, the addition of cholesterol tends to cause a reduction in the magnitude of these angles. The other data in Table II will be explained in the next two sections.

Orientational Order. The results tabulated in Table II show that for the DPH molecules $\lambda_2 \approx \lambda_4$, while for the TMA-DPH molecules $\lambda_2 > \lambda_4$. Consequently, the order parameters $\langle P_2 \rangle$ for the DPH molecules are significantly lower than those for the TMA-DPH probes in the same system, though similar values for $\langle P_4 \rangle$ are found. Inspection of Table II shows that in general the order parameters decrease with increasing unsaturation, for both probes. Surprisingly, however, the order parameters for DOPC bilayers without cholesterol are found to be significantly lower than those found in pure DLPC bilayers. The addition of cholesterol causes the order parameters to increase and to counteract the effects of the unsaturation of the fatty acid chains. However, it is interesting to note that the systems of DOPC, DLPC, and DGDG containing cholesterol exhibit virtually the same order parameters as the pure POPC bilayer system, irrespective of the probe molecule used.

In order to gain more insight into the orientational distribution of the probe molecules in the bilayer system, we have reconstructed the orientation distribution function $f(\beta)$, eq 4, using the $\langle P_2 \rangle$ and $\langle P_4 \rangle$ values listed in Table II. Figures 1 and 2 show the functions for DPH molecules embedded in

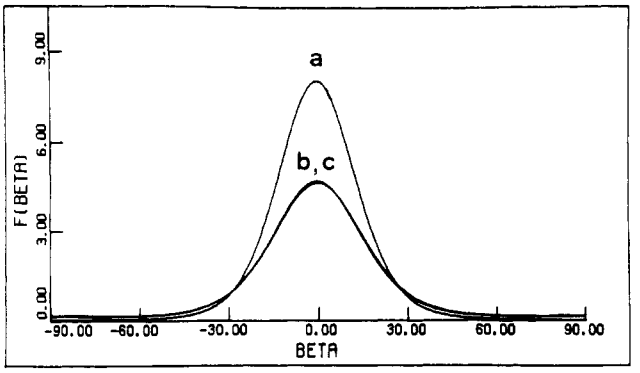

FIGURE 3: Orientational distribution functions of DPH molecules in multibilayers of POPC + cholesterol (a), DOPC + cholesterol (b), and DLPC + cholesterol (c).

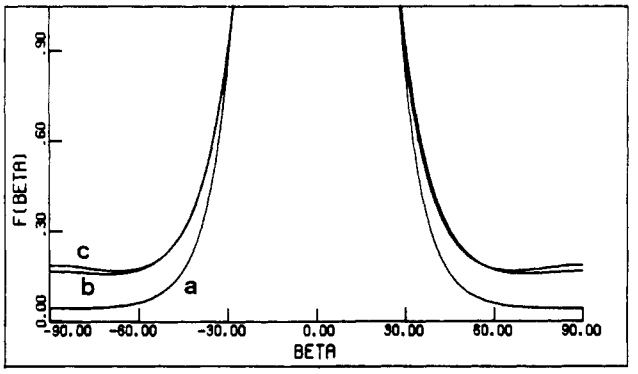

FIGURE 4: Orientational distribution functions of Figure 3 enlarged 10 times.

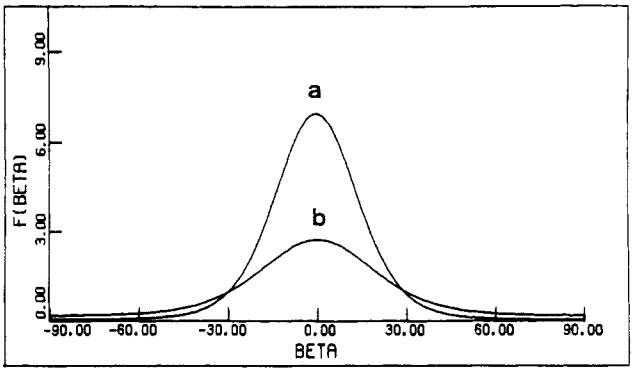

FIGURE 5: Orientational distribution functions of DPH molecules in multibilayers of POPC + stigmasterol (a) and DGDG + stigmasterol (b).

POPC, DOPC, and DLPC bilayers, respectively. The functions are plotted on the same vertical scale and give the probability of finding a molecule at a given orientation β. We note that the number density of the molecules is given by $\sin \beta f(\beta)$. All three functions exhibit a distinct minimum at $\beta \approx 60°$. This can be taken as a strong indication of the presence of at least two distinct populations of DPH molecules in the bilayers (Van Ginkel et al., 1986). Furthermore, the results indicate that 4–5% of the DPH molecules in POPC and DLPC bilayers lie with their long axes parallel to the surface of the bilayer. Surprisingly, this fraction increases to 13% in DOPC bilayers. The addition of cholesterol suppresses this effect (Figure 3 and 4) and narrows the orientational distribution of the DPH molecules. The influence of cholesterol is particularly marked in DOPC bilayers.

The effects of the addition of stigmasterol are less clear. While stigmasterol increases the molecular order of DPH molecules embedded in bilayers of POPC, it has the opposite

Table II: Analysis of AFD Measurements of DPH and TMA-DPH in Macroscopically Oriented Multibilayers of Different Lipids with and without Cholesterol or Stigmasterol and the Average Fluorescence Lifetimes of DPH and TMA-DPH in the Different Lipid Bilayers[a]

lipid + probe	λ_2	λ_4	β_ν (deg)	$D_\perp\langle\tau_f\rangle$	$\langle\tau_F\rangle$ (ns)[b]	$D_\perp$ (ns^{-1})	$\langle P_2\rangle$	$\langle P_4\rangle$	$f(90)/f(0)$ (%)	T (°C)
DMPC + DPH	2.41	0.69	24	0.369	8.21	0.045	0.60	0.31	1.7	35
POPC + DPH	1.75	1.06	30	0.249	7.45	0.033	0.52	0.30	3.7	21
DOPC + DPH	0.95	0.96	29	0.220	6.68	0.033	0.29	0.18	13	21
DLPC + DPH	1.58	0.90	41	0.171	6.90	0.025	0.45	0.25	5.3	21
DGDG + DPH	1.5	0.75	34	0.040			0.43	0.21	6	21
DMPC + chol + DPH			≈10				0.87			35
POPC + chol + DPH	2.93	1.22	14	0.301	7.09	0.042	0.74	0.47	0.5	21
DOPC + chol + DPH	1.83	0.96	21	0.230	7.11	0.032	0.52	0.29	3.5	21
DLPC + chol + DPH	1.70	1.06	15	0.286	6.86	0.042	0.51	0.29	4.0	21
DGDG + chol + DPH	1.89	0.65	24	0.170			0.50	0.24	4.0	21
DMPC + TMA	3.22	0.07	12	0.191	5.80	0.034	0.64	0.29	0.7	35
POPC + TMA	2.96	0.53	18	0.057	4.55	0.012	0.66	0.35	0.8	21
DOPC + TMA	2.41	0.18	19	0.082	2.96	0.028	0.54	0.21	2.4	21
DLPC + TMA	2.18	0.73	20	0.076	3.51	0.022	0.57	0.29	2.4	21
DGDG + TMA	2.27	0.12	17	0.041	2.60	0.016	0.51	0.18	3.0	21
DMPC + chol + TMA			15		5.80		0.93			35
POPC + chol + TMA	3.58	0.89	13	0.126	5.38	0.024	0.76	0.48	0.3	21
DOPC + chol + TMA	2.82	0.64	15	0.101	4.22	0.024	0.66	0.35	1.0	21
DLPC + chol + TMA	2.56	0.76	14	0.128	3.01	0.042	0.64	0.35	1.3	21
DGDG + chol + TMA	2.69	0.40	17	0.059	2.89	0.021	0.61	0.29	1.4	21
POPC + stigmast + DPH	2.97	0.29	18	0.235			0.71	0.42	0.6	21
DGDG + stigmast + DPH	1.58	0.46	32	0.110			0.40	0.16	7.0	21

[a] The analysis yields the following parameters: λ_2 and λ_4, coefficients in the equation for the anisotropic orienting potential $U(\beta)$ described under Theory; $\langle P_2\rangle$ and $\langle P_4\rangle$, second and fourth rank order parameters described under Theory; $D_\perp$, diffusion coefficients of the symmetry axis of the fluorescent probe molecule; β_ν, angle β between the absorption and emission moments of the fluorescent probes. The distribution functions $f(\beta)$ reconstructed from the calculated values of $\langle P_2\rangle$ and $\langle P_4\rangle$ allow determination of the fraction of probe molecules at 0° and 90°, respectively, with respect to the membrane plane. From these values the fraction $f(90)/f(0)$ can easily be calculated. [b] The given $\langle\tau_F\rangle$ values are the average values from different experiments.

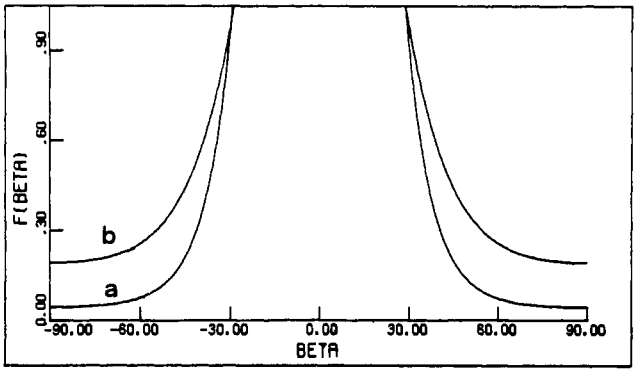

FIGURE 6: Orientational distribution functions of Figure 5 enlarged 10 times.

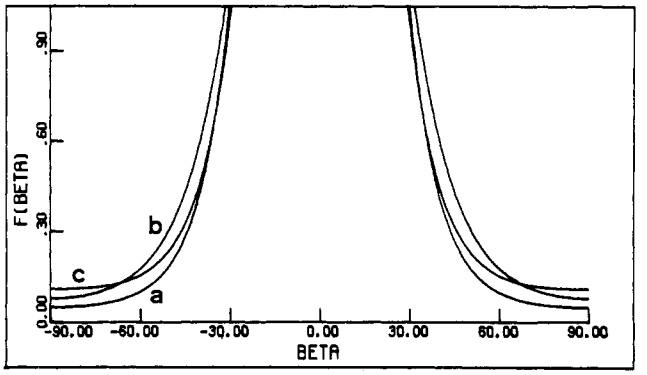

FIGURE 8: Orientational distribution functions of Figure 7 enlarged 10 times.

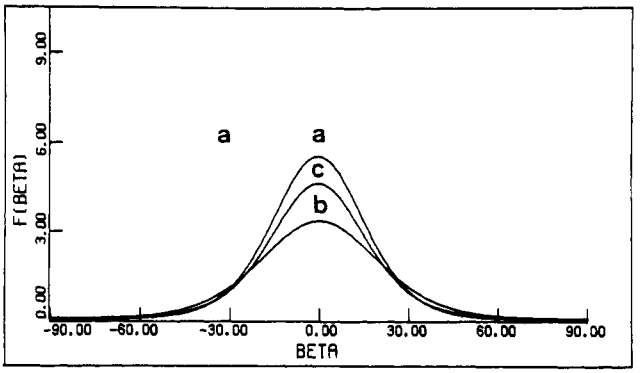

FIGURE 7: Orientational distribution functions of TMA-DPH molecules in multibilayers of POPC (a), DOPC (b), and DLPC (c).

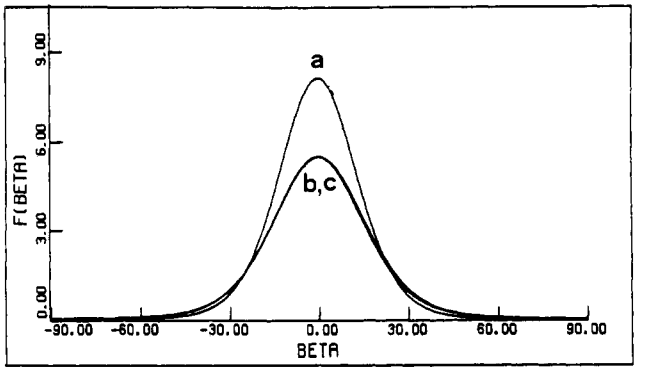

FIGURE 9: Orientational distribution functions of TMA-DPH molecules in multibilayers of POPC + cholesterol (a), DOPC + cholesterol (b), and DLPC + cholesterol (c).

effect in DGDG bilayers, Table II and Figures 5 and 6.

The orientational distribution functions for TMA-DPH molecules in POPC, DOPC, and DLPC bilayers are shown in Figure 7 and 8, respectively. In contrast with the distributions of the DPH molecules, the distribution functions for the TMA-DPH molecules decrease monotonically from a maximum at $\beta = 0°$ to $\beta = 90°$. We note further that only a small fraction of TMA-DPH in fact lies with their axes parallel to the bilayer surface. There is thus no evidence for heterogeneity in the distribution of these molecules in the bilayers. The influence of cholesterol is illustrated in Figures 9 and 10, and again an increase in the orientational order is obtained.

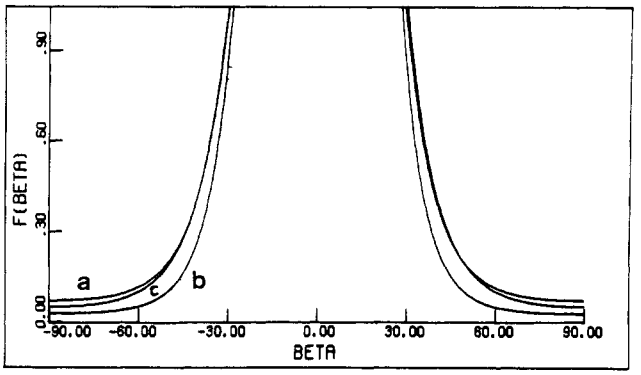

FIGURE 10: Orientational distribution functions of Figure 9 enlarged 10 times.

It is important to realize here that the results presented here are not sensitive to the transverse location of the probe molecules in the bilayer structure.

Reorientational Dynamics. The results in Table II show unambiguously that the values of $D_\perp$, the diffusion coefficient of the long molecular axis of the probe molecules, are considerably lower for the unsaturated bilayer systems at 21 °C (well above their phase transition temperatures) than for DMPC at 35 °C (T_c = 23 °C). This is particularly noticeable for the TMA-DPH molecules. Furthermore, we note that the DPH molecules reorientate faster than the TMA-DPH probes in the same system. Our results indicate further that the introduction of the first cis double bond has the greatest effect on the reorientation dynamics of the probe molecules.

A second, somewhat surprising result is that the addition of cholesterol into the bilayers causes the rates of reorientational motion of the probe molecules to increase significantly. The only exception is DOPC bilayers, where cholesterol appears to have only a small effect on the molecular dynamics.

Discussion

In the experiments presented below, DPH and TMA-DPH molecules were used to probe the molecular order and dynamics of bilayers of unsaturated lipids. The fluorescence depolarization techniques used monitor only the orientational order and reorientational dynamics independent of the transverse location of the probes in the bilayer structure. Nevertheless, the results are strongly indicative of a heterogeneous orientational distribution of DPH molecules in the pure lipid bilayers, which may be associated with a heterogeneity in the transverse disposition of the molecules. The orientational distribution functions are most easily rationalized in terms of a population of DPH molecules lying between the two lipid monolayers, with a second population interdigitated between the hydrocarbon chains. Such a picture is entirely consistent with earlier suggestions by Andrich and Vanderkooi (1976) and Lentz et al. (1976) that DPH molecules are preferentially located near the center of the bilayer. A similar conclusion was reached by Davenport et al. (1985) from measurements of energy transfer in vesicles of the unsaturated lipid egg PC. Our results show that the tendency of the DPH molecules to lie parallel to the bilayer surface increases with increasing unsaturation of the hydrocarbon chains and is counteracted by the addition of cholesterol. We note here that the analysis of fluorescence depolarization experiments is based on the assumption that the rate of motion of the molecules is independent of the absolute orientation of the molecules in the bilayer. Thus, the fraction of DPH molecules lying at the center of the bilayer is assigned the same dynamic behavior as those DPH molecules that are interdigitated between the hydrocarbon chains of the lipids. An analysis of the experimental data provided by the AFD experiments in terms of two populations of DPH molecules differing in their dynamic behavior cannot be justified in view of the extra free model parameters that enter the calculations. It is important to realize that our experiments afford the determination of a maximum of five independent quantities. The fact that our analysis yields a heterogeneous orientational population for DPH molecules is strongly suggestive that the results are not unequivocal.

In marked contrast, TMA-DPH molecules are expected to be anchored near the head groups of the lipids (Prendergast et al., 1981; Cranney et al., 1983; Donner & Stolz, 1985). The orientational distribution functions for TMA-DPH molecules presented below are consistent with such a hypothesis. The small probability for the probes to lie parallel to the surface of the bilayer is probably due to fluctuations in the lateral packing of the lipid molecules. A second possibility, which cannot be ruled out, is that these small effects are simply artifacts that arise from the reconstruction of the orientational distribution function from a limited knowledge of the order parameters. As already noted, only $\langle P_2 \rangle$ and $\langle P_4 \rangle$ can be determined experimentally, while the higher order parameters are estimated by the maximum entropy method.

Notwithstanding their transverse location in the bilayers, both probe molecules reveal the same trends in the effects of unsaturation and cholesterol on the orientational order in the bilayers. It is interesting that our results show that multibilayers of DOPC, DLPC, and DGDG containing cholesterol exhibit the same orientational order as multibilayers of pure POPC. We have, however, no explanation as yet for the anomalous behavior of the probe molecules in DOPC multilayers.

The orientational dynamics of the probe molecules revealed in our experiments are at odds with previous investigations on the effects of increasing unsaturation of the lipid chains (Seelig & Seelig, 1977; Stubbs et al., 1980, 1981). While these authors reported an increase in the reorientational rates, our results indicate the opposite. Furthermore, our findings that the addition of cholesterol causes an increase both in the orientational ordering and in the rates for the reorientational motions of the probe molecules conflict with current concepts of membrane fluidity at first introduced by Chapman et al. (1966). According to this concept, the introduction of unsaturation into the lipid hydrocarbon chains reduces the molecular ordering and increases the chain motions so that the membranes become "more fluid". Cholesterol, on the other hand, reverses this effect.

The question now arises whether the model for the molecular reorientation motion has any bearing on our results. We have, however, previously shown (Mulders et al., 1986; Van de Ven & Levine, 1984) that the strong collision model, where the molecules are assumed to undergo random uncorrelated jumps, yields results similar to those obtained from the rotational diffusion model. In marked contrast, the results from AFD experiments cannot be described in terms of the popular "wobble-in-cone" model. This has been ascribed by us previously (Van de Ven & Levine, 1984) to the fact that the model predicts negative values for the order parameter $\langle P_4 \rangle$ for the range of values of $\langle P_2 \rangle$ observed. In order to gain more insight into the failure of the wobble-in-cone model, it is important to bear in mind that the three time-averaged correlation functions g_0, g_1, and g_2 are determined separately in the AFD experiments. On the other hand, the fluorescence anisotropy $\bar{r}$ obtained from experiments on vesicle systems is given

by the sum $\bar{r} = g_0 + 2g_1 + 2g_2$ in steady-state experiments or $r(t) = G_0(t) + 2G_1(t) + 2G_2(t)$ in time-resolved experiments (Szabo, 1984; Zannoni et al., 1983). Comparison of the analyses using for example the rotational diffusion and the wobble-in-cone models shows that different numerical values can be given to the correlation functions g_k or $G_k(t)$, but in such a way that the fluorescence anisotropy $\bar{r}$ or $r(t)$ remains constant (Van Langen et al., 1987). Indeed, these authors demonstrated that the time-resolved fluorescence anisotropy of DPH and TMA-DPH in POPC vesicles, with or without cholesterol, can be interpreted in terms of two completely different sets of order parameters and rotational diffusion coefficients. The two solutions were found to be statistically equivalent. The results corresponding to the wobble-in-cone model show that the diffusion coefficients of DPH and TMA-DPH decrease markedly on the addition of cholesterol. On the other hand, the second solution which corresponds closely to the AFD results reported above indicates that a significant increase in the diffusion coefficients is induced by the presence of cholesterol.

Time-resolved fluorescence anisotropy studies of DPH molecules in vesicles of unsaturated lipids have been reported by Stubbs et al. (1980, 1981). These authors used the wobble-in-cone model in the analysis of the experiments together with the simplified assumption that the time-dependence of the anisotropy can be treated as an effective monoexponential decay. The discrepancies between their results and the ones presented here may well be due in large measure to the deficiencies of the wobble-in-cone model analysis. Indeed, similar experiments carried out in our laboratory (Van Langen et al., 1987) and analyzed with the rotational diffusion model confirm the general trends obtained from the AFD experiments. It is interesting to note in this context that our AFD results are also corroborated by ESR studies of cholestane spin-labels incorporated into multibilayers of DMPC, POPC, and DGDG (Koole et al., 1984; Van Ginkel et al., 1986). Nevertheless, the discrepancies in the molecular dynamics of fluorescent probe molecules embedded in lipid vesicles and the flat multibilayer systems suggest that the curvature of the bilayer planes plays an important role in determining the behavior of the probe molecules. This is indeed not surprising in view of the known differences in physical properties such as phase transitions between vesicle and multilamellar samples.

The discussion above gives a clear signal that the concept of membrane fluidity must be used with some caution. This term can be misleading since in common use changes in fluidity are always associated with changes in viscosity. We thus support the earlier suggestion of Seelig and Seelig (1977) that in considering the dynamic structure of lipid bilayers a clear distinction must be made between molecular orientational order and the reorientational dynamics.

ACKNOWLEDGMENTS

We thank Dr. D. Shaw and Dr. M. Martin for their assistance during the measurements. H.v.L. was supported by the Dutch Foundation for Biophysics under the auspices of the Netherlands Organization for Pure Research (ZWO). The use of the SRS in Daresbury (England) was made possible by ZWO in connection with the agreement between SERC and ZWO.

REFERENCES

Andrich, M. P., & Vanderkooi, J. M. (1976) *Biochemistry 15*, 1257–1261.

Chapman, D., Byrne, P., & Shipley, G. G. (1966) *Proc. R. Soc. London, A 290*, 115–142.

Cranney, M., Cundall, R. B., Jones, G. R., Richards, J. T., & Thomas, E. W. (1983) *Biochim. Biophys. Acta 735*, 418–425.

Cullis, P. R., & De Kruijff, B. (1979) *Biochim. Biophys. Acta 559*, 399–420.

Dale, R. E. (1980) in *Time-Resolved Fluorescence Spectroscopy in Biochemistry and Biology* (Cundall, R. B., & Dale, R. E., Eds.) pp 555–604, Plenum, New York and London.

Dale, E., Chen, L. A., & Brand, L. (1977) *J. Biol. Chem. 252*, 7500–7507.

Davenport, L., Dale, R. E., Bisby, R. H., & Cundall, R. B. (1985) *Biochemistry 24*, 4097–4108.

Demel, R. A., Bruckdorfer, K. R., & Van Deenen, L. L. M. (1972a) *Biochim. Biophys. Acta 255*, 321–330.

Demel, R. A., Geurts van Kessel, W. S. M., & Van Deenen, L. L. M. (1972b) *Biochim. Biophys. Acta 266*, 26–40.

Donnor, M., & Stoltz, J. F. (1985) *Biorheology 22*, 385–397.

Dufourc, E. J., & Smith, I. C. P. (1986) *Chem. Phys. Lipids 41*, 123–135.

Dufourc, E. J., Parish, E. J., Chitrakorn, S., & Smith, I. C. P. (1984) *Biochemistry 23*, 6062–6071.

Ghosh, R., & Seelig, J. (1982) *Biochim. Biophys. Acta 691* 151–160.

Guyer, W., & Bloch, K. (1983) *Chem. Phys. Lipids 33*, 312–322.

Hildenbrand, K., & Nicolau, C. (1979) *Biochim. Biophys. Acta 553*, 365–377.

Huang, C. (1977) *Lipids 12*, 348–356.

Johansson, L. B. Å. (1985) *Chem. Phys. Lett. 118*, 516–521.

Johansson, L. B. Å., & Lindblom, G. (1980) *Q. Rev. Biophys. 13*, 63–118.

Kawato, S., Kinosita, K., & Ikegami, A. (1978) *Biochemistry 17*, 5026–5031.

Koole, P., Dammers, A. J., Van Ginkel, G., & Levine, Y. K. (1984a) *Biochim. Biophys. Acta 777*, 297–305.

Koole, P., Dammers, A. J., & Levine, Y. K. (1984b) *Chem. Phys. Lipids 35*, 161–170.

Kooyman, R. P. H., Vos, M. H., & Levine, Y. K. (1983) *Chem. Phys. 81*, 461–472.

Kusumi, A., Subczynski, W. K., Pasenkiewicz-Gierula, M., Hyde, J. S., & Merkle, H. (1986) *Biochim. Biophys. Acta 854*, 307–317.

Kutchai, H., Chandler, L. H., & Zavoico (1983) *Biochim. Biophys. Acta 736*, 137–149.

Lax, M., & Nelson, D. F. (1973) in *Coherence and Quantum Optics* (Mandel, L., & Wolf, E., Eds.) pp 415–445, Plenum, New York.

Lentz, B. R., Barenholz, Y., & Thompson, T. E. (1976) *Biochemistry 15*, 4521–4528.

McKersie, B. D., & Thompson, J. E. (1979) *Plant Physiol. 63*, 802–805.

Mulders, F., Van Langen, H., Van Ginkel, G., & Levine, Y. K. (1986) *Biochim. Biophys. Acta 859*, 209–218.

Oldfield, E., Meadows, M., Rice, D., & Jacobs, R. (1978) *Biochemistry 17*, 2727–2740.

Prendergast, F. G., Haugland, R. P., & Callahan, P. J. (1981) *Biochemistry 20*, 7333–7338.

Quinn, P. J., & Chapman, D. (1980) *Critical Reviews in Biochemistry* (Fasman, G. D., Ed.) CRC, Boca Raton, FL.

Rose, M. F. (1957) *Elementary Theory of Angular Momentum*, Wiley, New York.

Seelig, A., & Seelig, J. (1975) *Biochim. Biophys. Acta 406*, 1–5.

Seelig, A., & Seelig, J. (1977) *Biochemistry 16*, 45–50.

Seelig, J., & Waespe-Sarčevic, N. (1978) *Biochemistry 17*, 3310-3315.
Seelig, J., & Seelig, A. (1980) *Q. Rev. Biophys. 13*, 19-61.
Smutzer, G., & Yeagle, P. L. (1985) *Biochim. Biophys. Acta 814*, 274-280.
Stockton, G. W., & Smith, I. C. P. (1976) *Chem. Phys. Lipids 17*, 251-263.
Stubbs, C. D. (1983) *Essays Biochem. 19*, 1-39.
Stubbs, C. D., Tsang, W. M., Belin, J., Smith, A. D., & Johnson, S. M. (1980) *Biochemistry 19*, 2756-2762.
Stubbs, C. D., Kouyama, T., Kinosita, K., & Ikegami, A. (1981) *Biochemistry 20*, 4257-4262.
Szabo, A. (1984) *J. Chem. Phys. 81*, 150-167.
Van der Meer, B. W., Vos, M. H., & Levine, Y. K. (1983) *Chem. Phys. 66*, 39-50.
Van de Ven, M. J. M., & Levine, Y. K. (1984) *Biochim. Biophys. Acta 777*, 283-296.
Van de Ven, M. J. M., Van Ginkel, G., & Levine, Y. K. (1984) *Biochem. Biophys. Res. Commun. 123*, 352-357.
Van Ginkel, G., Korstanje, L. J., Van Langen, H., & Levine, Y. K. (1986) *Faraday Discuss. Chem. Soc. 81*, 49-61.
Van Langen, H., Levine, Y. K., Ameloot, M., & Pottel, H. (1987) *Chem. Phys. Lett. 140*, 394-400.
Veatch, W. R., & Stryer, L. (1977) *J. Mol. Biol. 117*, 1109-1113.
Wolber, P. K., & Hudson, B. S. (1981) *Biochemistry 20*, 2800-2810.
Worcester, D. L., & Franks, N. P. (1976) *J. Mol. Biol. 100*, 359-378.
Yeagle, P. L. (1981) *Biochim. Biophys. Acta 640*, 263-273.
Yeagle, P. L. (1985) *Biochim. Biophys. Acta 822*, 267-287.
Zannoni, C. (1979) *Mol. Phys. 83*, 1813-1827.
Zannoni, C., Arcioni, A., & Cavatorta, P. (1983) *Chem. Phys. Lipids 32*, 179-250.

Causes of Nondiffusing Lipid in the Plasma Membrane of Mammalian Spermatozoa†

David E. Wolf,* Adrienne C. Lipscomb, and Valerie M. Maynard

Endocrine Reproductive Biology Group, Worcester Foundation for Experimental Biology, 222 Maple Avenue, Shrewsbury, Massachusetts 01545

Received May 4, 1987; Revised Manuscript Received September 18, 1987

ABSTRACT: In the plasma membranes of most mammalian somatic cells, lipid is nearly completely free to diffuse laterally in the plane of the membrane. In mammalian spermatozoa and certain other highly polarized mammalian cells, a significant fraction of the plasma membrane lipid is not free to diffuse laterally. Using the technique of fluorescence recovery after photobleaching, we have demonstrated that a variety of fluorescent lipid analogues exhibit a nondiffusing fraction in the plasma membrane of the anterior region of the ram sperm head. The possible causes of this nondiffusing fraction were investigated. The nondiffusing lipid fraction is not the result of lipid oxidation during handling, and it is not released by extensive enzymatic digestion of the membrane surface proteins or the "blebbing" of the membrane by hypoosmotic shock. When lipid bilayers were prepared from protein-free lipid extracts of the plasma membranes of spermatozoa, most of the nondiffusing fraction was retained. These results suggest that the nondiffusing lipid fraction results from lipid factors such as lateral phase separations, which can cause such a nondiffusing fraction in model systems.

Fluorescence recovery after photobleaching (FPR)[1] measurements show that, in the plasma membrane of most somatic cells, lipid is nearly completely free to diffuse laterally in the plane of the membrane [for reviews, see Peters (1981) and Edidin (1981)]. In contrast, the plasma membranes of mammalian spermatozoa have large nondiffusing lipid fractions (Wolf & Voglmayr, 1984; Wolf et al., 1986a,c). This nondiffusing lipid pool develops during spermiogenesis (Wolf et al., 1986c) and becomes an increasingly larger portion of total plasma membrane lipid as the sperm further differentiate during epididymal maturation (Wolf & Voglmayr, 1984) and capacitation (Wolf et al., 1986a). The fraction of nondiffusing lipid in mature sperm can exceed 50%, which is far greater than the 10-15% observed in most somatic cell plasma membranes (Axelrod, 1979). This may be related to the highly polarized nature of the mammalian spermatozoa (Friend, 1982), since significant immobile lipid has been observed only in other highly polarized mammalian cells, such as those of epithelia (Weaver, 1985) and endothelia (Nakache et al., 1985).

† This work was supported in part by National Institutes of Health Grant HD 17377 (to D.E.W.) and by private grants from the A. W. Mellon and E. J. Noble Foundations, as well as the Educational Foundation of America, to the Worcester Foundation. Part of this work was completed while A.C.L. was a summer research fellow from Mt. Holyoke College. We thank the Alden Trust for support of this program. A preliminary report of this work was presented at the Testis Workshop in October 1986 at Nashville, TN.

* Author to whom correspondence should be addressed.

[1] Abbreviations: BSA, bovine serum albumin; $C_N$diI, 1,1′-dialkyl-3,3,3′,3′-tetramethylindocarbocyanine perchlorate (N = alkyl chain length); D, diffusion coefficient; FPR, fluorescence recovery after photobleaching; NBD, 7-nitro-2,1,3-benzoxadiazol-4-yl; NBD-PC(6), NBD acyl chain labeled phosphatidylcholine; NBD-PE, NBD amino labeled phosphatidylethanolamine; PBS, phosphate-buffered saline with 1.2 mM Ca^{2+} and 5 mM Mg^{2+}; % R, percent recovery; TES, 2-[[tris(hydroxymethyl)methyl]amino]ethanesulfonic acid.

0006-2960/88/0427-0860$01.50/0